Blind infrared spectroscopic data restoration with the similarity of multi-scales regularization

Hai Liu, *Member, IEEE*, Zhaoli Zhang*, Sanyan Liu*, Jiangbo Shu, and Zhi Liu
National Engineering Research Center for E-Learning, Central China Normal University, Wuhan, 430079, P.R. China
Email: zl.zhang@mail.ccnu.edu.cn and lsy5918@mail.ccnu.edu.cn

***Abstract*- Band overlap and random noise exist widely when the spectra are captured using an infrared spectrometer, especially when the problems of instrument aging has become more and more serious recently. In this paper, via introducing the similarity of multiscales, a blind spectral deconvolution method is proposed. Considering similarity of the latent spectrum between different scales, it is used as a prior to constrain the estimated latent spectrum similar to pre-scale to reduce artifacts which is produced from deconvolution. Experiments indicate that the proposed method is able to obtain better performance than the state-of-the-art methods, and obtain satisfying deconvolution results with fewer artifacts. The recovered infrared spectra can easily extract the spectral features and recognize the unknown objects.**

***Keywords:* Spectral restoration, Multiscales, Blind deconvolution, Infrared spectroscopic data.**

I. INTRODUCTION

Infrared spectroscopic data often suffer from the band overlap and random noise [1] (such as Fig. 1), which limit the development of spectroscopy in industrial and commercial applications, such as rapid identification of chemicals [1, 2], and physical properties of small molecules [3, 4], feature extraction [5, 6], material recognition [7, 8]. The spectra overlap are usually modeled as a linear degradation system,

$$\boldsymbol{b}=\boldsymbol{l}\otimes\boldsymbol{k}+\boldsymbol{n}, \quad (1)$$

where $\boldsymbol{b}$ is the degraded spectrum, $\boldsymbol{l}$ is the latent spectrum, $\boldsymbol{n}$ is the additive noise usually assumed as Gaussian distribution, $\otimes$ is the convolution operator. And the symbol $\boldsymbol{k}$ is the instrument function, which is usually assumed to be linear shift-invariant. The goal of spectral deconvolution is to recover the latent spectrum $\boldsymbol{l}$ from the observed degraded spectrum $\boldsymbol{b}$.

During the past two decades, deconvolution has become one of effective mathematical technique to solve the degraded problem [9, 10]. In sum, all the deconvolution methods for spectroscopic data can be divided into three types: the non-blind deconvolution (NBD) method [11, 12] with the known instrument function, semi-blind deconvolution (SBD) [13, 14] method with the parametrically modeled instrument function, and the blind deconvolution (BD) [15] method with unknown instrument function. Because the instrument function is hardly known when the degraded spectrum captured using an infrared spectrometer, we only concern the blind case in this paper. Some researchers use a blackbody to capture spectrum in order to measure the instrument function, and then estimate the latent spectrum using the NBD method; however, the instrument function often changes over time.

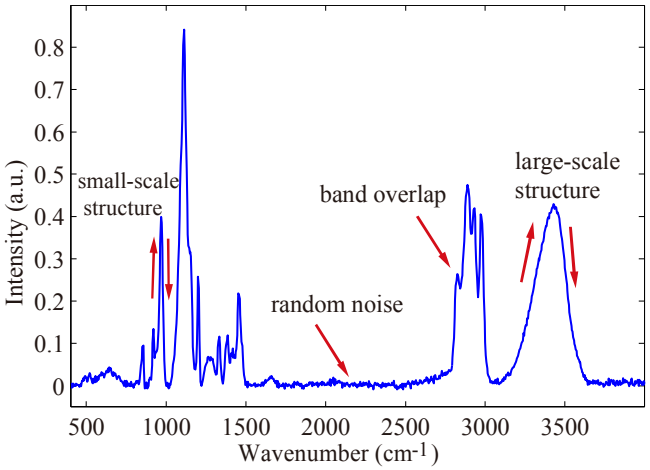

Fig. 1. Infrared spectrum of 1-methoxy-2-propanol ($C_4H_{10}O_2$). The infrared spectroscopic data often suffer from the band overlap and random noise. It includes small-scale structure and large-scale structure.

The BD methods have been proposed in recent years [13, 14, 16], and these methods almost employ the deconvolution method to remove band overlap. Because the deconvolution problem is an ill-posed problem, it always results in the deconvolution result with artifacts. In order to eliminate the influence of the artifacts and get a satisfying spectrum, many deconvolution methods via introducing different priors and regularization terms have been proposed, such as Fourier-self deconvolution (FSD) [12], Tikhonov regularization [13, 17], total variation [18], high order statistics [16], entropy regularization [19], sparsity regularization [20-22]. With those useful priors and regularizations, all the methods have achieved impressive results. However, they only consider the prior information in their own scales, and their deconvolution ability is limited. In this paper, we proposed a new method to address those.

The outline of the paper is organized as follows. In the next section, we describe the spectral observations. And in the Section III, the proposed model is illustrated, namely, spectrum deconvolution method with the similarity of the multiscales regularization. The optimization algorithm for the proposed method is presented in Section IV. Some results and discussions are given in Section V, followed by a brief conclusion section.

II. SPECTRAL OBSERVATIONS

First, we examined the original infrared spectral data and its downsampled versions (in Fig. 2). Then, we obtained the

following interesting observations: (1) Both large-scale structure and small-scale structure existed in the degraded spectrum. They take up difference wavenumber length; (2) The more spectral resolution downsamples, the less small-scale structure leaves. These can be shown in Fig. 2.

Inspired by these observations, we proposed a novel blind spectral deconvolution method which uses the similarity of the multiscales. We first downsample degraded spectrum to multiscales, and then restore spectrum at each scale. Considering that the latent spectrum is similar between adjacent scales, the deconvolution result of the pre-scale is treated as a prior of current scale in order to reduce the artifacts. The proposed method uses the information of the pre-scale sufficiently. In order to reduce the artifacts, not only the instrument function of the pre-scale is propagated to the current scale as a initial value, but also the latent spectrum of the pre-scale is used as a constrain in current scale.

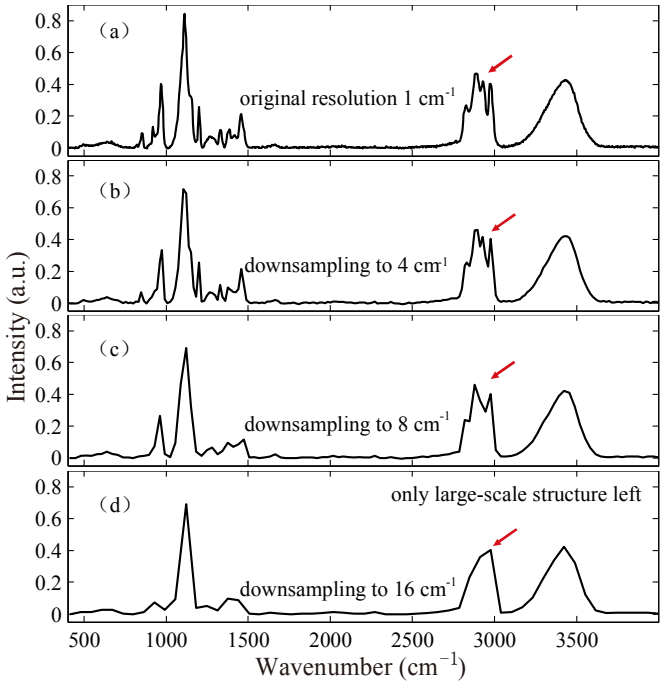

Fig. 2. Spectra are similar between adjacent scales. Degraded spectrum is downsampled to each scale. The more spectral resolution downsamples, the less small-scale structure leaves.

III. PROPOSED METHOD

The degraded spectrum is first downsampled to each scale. The corresponding instrument function is also downsampled with the degraded spectrum downsampling to small scale, so each downsampled degraded spectrum is a less overlap version than the original observed spectrum. When using the tradition method, the latent spectrum is easily estimated and with less artifacts under the less overlap version, and the latent spectrum with more artifacts with the scale increasing. It is worth noting that the latent spectrum is similar to the adjacent scales, so we used the estimated latent spectrum of pre-scale, which is with less artifacts, as a constraint when the latent spectrum of current scales is estimated in order to reduce the artifacts. The details of the proposed method is described as Fig. 2.

In the blind spectral deconvolution problem, we have to estimate the instrument function $\boldsymbol{k}$ and latent spectrum $\boldsymbol{l}$ from the degraded spectrum $\boldsymbol{b}$. The blind spectrum deconvolution method always stabilizes the solution via regularization as the following framework:

$$\{\boldsymbol{k},\boldsymbol{l}\}=\arg\min_{\boldsymbol{k},\boldsymbol{l}}\{\|\boldsymbol{b}-\boldsymbol{k}\otimes\boldsymbol{l}\|_2^2+\alpha\rho(\boldsymbol{l})+\gamma\rho(\boldsymbol{k})\} \quad (2)$$

where $\rho(\boldsymbol{l})$ and $\rho(\boldsymbol{k})$ are the regularization terms of $\boldsymbol{l}$ and $\boldsymbol{k}$ respectively. In this paper, the similarity between adjacent scales and sparseness prior of the latent spectra are used as the regularization term of $\boldsymbol{l}$, and L_2-norm has been used as the regularization term of $\boldsymbol{k}$.

Considering the similarity between adjacent scales, we first downsample the degraded spectrum as follows:

$$\boldsymbol{b}_{\mathrm{i}}=\mathbf{D}\boldsymbol{b}_{\mathrm{i-1}}, \quad (3)$$

where $\boldsymbol{b}_{\mathrm{i}}$ is the downsampled degraded spectrum in the i-th scale, and $\mathbf{D}$ is the downsampled operator. The small subscript i is corresponding to the spectral length, and the $\boldsymbol{b}_0$ is the original spectrum. Obviously the latent spectrum $\boldsymbol{l}$ and the instrument function $\boldsymbol{k}$ should also be downsampled in the corresponding scale as $\boldsymbol{l}_{\mathrm{i}}=\mathbf{D}\boldsymbol{l}_{\mathrm{i-1}}$ and $\boldsymbol{k}=\mathbf{D}\boldsymbol{k}_{\mathrm{i-1}}$. Then combining with the sparse prior of the latent spectrum, the formulation under each scale could represent as follows:

$$\{\boldsymbol{k}_i,\boldsymbol{l}_i\}=\arg\min_{\boldsymbol{k},\boldsymbol{l}}\{\|\boldsymbol{b}-\boldsymbol{k}\otimes\boldsymbol{l}\|_2^2+\alpha\|\nabla[\boldsymbol{l}_i-\boldsymbol{l}_{i'}]\|_2^2+\beta\|\nabla\boldsymbol{l}_i\|^\eta+\gamma\|\boldsymbol{k}_i\|_2^2\} \quad (4)$$

where η=0.6 is the hyper-Laplacian coefficient, the α, β, and γ are the regularization parameters, and ∇ present the gradient operator. $\boldsymbol{l}_{\mathrm{i}}=(\mathbf{D}^*)\boldsymbol{l}_{\mathrm{i+1}}$, and $\mathbf{D}^*$ is upsampling operator which is the adjoint operator of $\mathbf{D}$. We explain each term of the model in detail as follows.

(1) The first term is the reconstruction constraint, i.e., the deconvolution spectrum should be consistent with the observation degradation model.

(2) The second term constrains the latent spectrum similarity with the latent spectrum of the pre-scale;

(3) The third term is the sparse prior of gradient spectrum assumed to follow the hyper-Laplacian distribution;

(4) The forth term is a L_2-norm based regularization term to stabilize the instrument function estimation.

The basic idea of the unified model is to make full use of the similarity between adjacent scales and preserve the multiscales structural information; meanwhile, the deconvolution spectrum should have a sparse representation. In this paper, the proposed model is called as Blind Deconvolution with the Similarity of Multiscales regularization (BD-SMR).

IV. OPTIMIZATION

The proposed model (4) involves non-smooth term and is hard to minimize directly. We first downsample the observation spectrum to each scale, then use Eq. (4) to estimate latent spectrum and instrument function at each scale, until the scale equals original resolution. The Eq. (4) can be minimized using the alternation minimization (AM) algorithm.

A. Instrument function estimation

In this subsection, we estimate the blur kernel $\boldsymbol{k}_i$ via fixing the latent spectrum $\boldsymbol{l}_i$, and the object function Eq. (4) reduces to the following one:

$$\boldsymbol{k}_i = \arg\min_{\boldsymbol{k}} \{\| \boldsymbol{b} - \boldsymbol{k} \otimes \boldsymbol{l} \|_2^2 + \gamma \| \boldsymbol{k}_i \|_2^2\} \tag{5}$$

which is a least square problem with Tikhonov regularization, thus, it leads to a closed form solution:

$$\boldsymbol{k}_i = F^{-1}\left(\frac{\overline{F(\boldsymbol{l}_i)} \circ F(\boldsymbol{b}_i)}{\overline{F(\boldsymbol{l}_i)} \circ F(\boldsymbol{l}_i) + \gamma \boldsymbol{I}} \right) \tag{6}$$

where $F(\bullet)$ and $F^{-1}(\bullet)$ are 1D FFT (fast Fourier transform) operator and IFFT operator respectively. $\overline{F(\bullet)}$ is the conjugated of $F(\bullet)$. I denotes the identity matrix and the symbol ° presents element-wise multiplication. The numerical integral of $\boldsymbol{k}$ is normalized to 1.

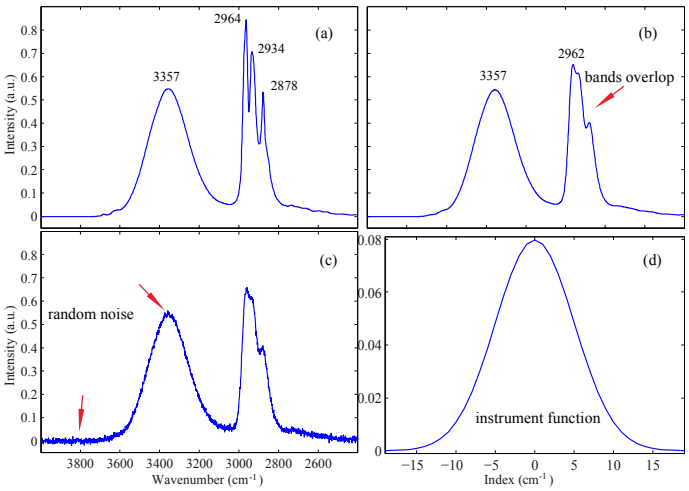

Fig. 3. Degraded infrared spectrum simulation. (a) Ground-truth infrared spectrum of 3-Pentanol ($C_5H_{12}O$). (b) Convolution with the IRF (Fig. 3(d)). (c) Contaminated by Gaussian noise. (d) Instrument function (Gaussian function).

B. Latent spectrum estimation

In this step, we fix $\boldsymbol{k}$ and optimize $\boldsymbol{l}$. The object functional Eq. (4) can be represented as

$$\boldsymbol{l}_i = \arg\min_{\boldsymbol{k},\boldsymbol{l}} \{\| \boldsymbol{b} - \boldsymbol{k} \otimes \boldsymbol{l} \|_2^2 + \alpha \| \nabla[\boldsymbol{l}_i - \boldsymbol{l}_i] \|_2^2 + \beta \| \nabla \boldsymbol{l}_i \|^{0.6}\} \tag{7}$$

Which` is non-convex on IR. The iteratively reweighted least squares (IRLS) method is employed to optimize it.

$$\boldsymbol{l}_i = \arg\min_{\boldsymbol{k},\boldsymbol{l}} \{\| \boldsymbol{b} - \boldsymbol{k} \otimes \boldsymbol{l} \|_2^2 + \alpha \| \nabla[\boldsymbol{l}_i - \boldsymbol{l}_i] \|_2^2 + \beta \omega(\nabla \boldsymbol{l}_i) \| \nabla \boldsymbol{l}_i \|_2^2\} \tag{8}$$

$$\omega(\nabla \boldsymbol{l}_i) = | \nabla \boldsymbol{l}_i |^{0.6-2} \tag{9}$$

When $\boldsymbol{k}$ is fixed, Eq. (9) can be optimized using the conjugate gradient method.

The regularization parameters α, β, γ are discussed as our previous work [13]. From the large-scale simulation experiments, the parameters are suggested as $\alpha \in [0.001,0.006]$, $\beta \in [0.01,0.1]$, $\gamma \in [200,400]$. We declare convergence when for more than two consecutive iterations both the instrument function and latent spectrum changes less than threshold values: $\| \boldsymbol{l}^{n+1} - \boldsymbol{l}^n \| / \| \boldsymbol{l}^n \| < d_1$ and $\| \boldsymbol{h}^{n+1} - \boldsymbol{h}^n \| / \| \boldsymbol{h}^n \| < d_2$, where d_1 and d_2 are predetermined coefficients. The deconvolution procedure described in this section is summarized as follows:

Algorithm 1. Spectral deconvolution using the similarity of multiscales regularization

Input: Degraded spectrum $\boldsymbol{b}$, downsampling spectrum: $\boldsymbol{b}_1$, $\boldsymbol{b}_2$, …, $\boldsymbol{b}_s$

1: Select α, β, and γ

2: Initialize multiscales number s=4 (this paper).

3: While : $\| \boldsymbol{l}^{n+1} - \boldsymbol{l}^n \| / \| \boldsymbol{l}^n \| < d_1$ and $\| \boldsymbol{h}^{n+1} - \boldsymbol{h}^n \| / \| \boldsymbol{h}^n \| < d_2$

(i) Fix $\boldsymbol{l}^{n+1}=\boldsymbol{l}^n$, solve Eq. (5) via (6);

(ii) Fix $\boldsymbol{k}^{n+1}=\boldsymbol{k}^n$, solve Eq. (8) using the iteratively reweighted least squares method (IRLS);

Output: estimated latent spectrum $\boldsymbol{l}$, instrument function $\boldsymbol{k}$.

In this paper, the symbols d_1 and d_2 are the predetermined coefficients between 10^{-9} and 10^{-7}.

V. EXPERIMENTS

In our tests, simulated and real spectra were used to verify the proposed method. All the test spectra were normalized to [0, 1]. Three spectral deconvolution methods, the Fourier-self deconvolution method (FSD) [11], semi-blind deconvolution method (SBD) [13] and blind deconvolution with adaptive total variation method (BD-ATV) [18] were compared. In order to give an overall evaluation, five quantitative indexes are employed. The indices include the correlation coefficient (CC), weighted correlation coefficient (WCC) [23], full width at half-maximum ratio (FWHMR) $\frac{1}{N}\sum_i^N FWHM_b^{(i)} / FWHM_l^{(i)}$, and noise amplification ratio (NAR) $\sum |\nabla \boldsymbol{l}| / |\nabla \boldsymbol{b}|$ [24, 25]. Among these indexes, the CC and WCC require the existence of a reference spectrum. Thus, it can only be used in simulated experiments. The FWHMR and NAR, which are non-reference indexes, which can also be used in real spectral experiments. It has been verified that the two metrics can reflect the width reduction and noise suppression [24]. The larger the value of FWHMR and NAR, the higher the spectral quality.

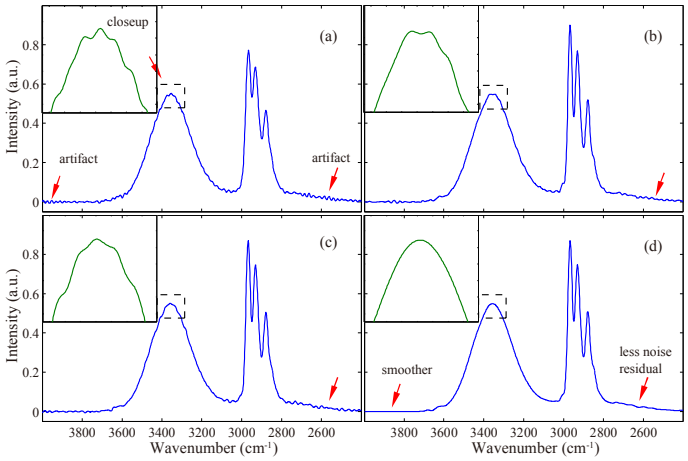

Fig. 4. Simulated experiment results. (a) FSD method [11]. (b) SBD method [13]. (c) BD-ATV method [18]. (d) Proposed method.

A. Simulated Experiments

In simulated experiments, we selected the three infrared spectra captured by the Fourier transform infrared spectrometer. Only the experimental result of infrared spectrum of 3-Pentanol ($C_5H_{12}O$) is shown here. Original

spectrum (Fig. 3(a)) was degraded by the instrument function of Gaussian function with standard deviation σ=9 (Fig. 3(d)), then the overlap spectrum was further contaminated with Gaussian noise (Fig. 3(c)). First, we consider the infrared spectrum of 3-Pentanol ($C_5H_{12}O$) from 4000 to 2500 cm^{-1}. In this experiments, we set the parameters as α=0.002, β=0.07, γ=300 and 120 iterations. For the FSD method, the narrowing factor k=1.37. For the SBD and BD-ATV methods, the regularization parameters are set as the references.

Table I. Band distortions (Fig. 4) in deconvoluted spectra by FSD, SBD and MOBSD methods.

Band positions		3357	2964	2934	2878	RMSE
Height	FSD	-0.051[a]	-0.109	-0.086	-0.123	0.0093
	BD-ATV	-0.014	+0.016	-0.035	-0.131	0.0047
	BD-SMR	-0.011	+0.012	-0.027	+0.101	**0.0028**
Position	FSD	-2	+1	-3	+1	3.75
	BD-ATV	+1	-1	-2	+2	2.50
	BD-SMR	+1	+2	0	-1	**1.50**

[a] plus or minus symbol indicates larger or smaller than the original respectively.

The experimental results are shown in Fig. 4. All the methods can split the overlap peak at 2962 cm^{-1} (Fig. 3(b)). Residual noise can be observed in Fig. 4(a). Comparing Fig. 4(d) with Figs. 4(a)-(c), it can be seen that the peak at 3357 cm^{-1} is smoother than other results. Their closeups are shown in the top-left corner. The RMSE of band distortions, their positions and height are compared in Table 1. The comparison shows that the BD-SMR result is the most similar one to the original spectrum. This is because the compared methods do not consider the similarity in multiscales. On the contrary, owing to the second term in our method, the band detail information are well preserved.

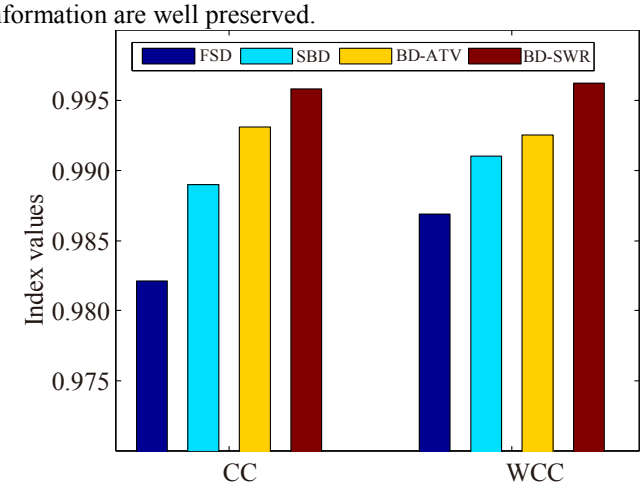

Fig. 5. Values of CC and WCC in Fig. 4. The larger the values, the similar to the original spectrum.

The reference evaluation results are shown in Fig. 5. It is seen that, the values of the CC and WCC indices of the proposed method are higher than those of the other methods. It can be seen that the FWHMR and NAR indices have a similar trend to the CC and WCC indices, which validate the good performance of the no-reference indices. Thus, it is used to evaluate the deconvolution results of the real spectra in the next section. Other two degraded spectrum cases are also tested, which are shown in Table II.

Table II. Comparisons of FWHMR and NAR by different methods on the Dihexylamine IR spectrum. The larger the merits value, the higher the spectral quality.

Indices	Spectra	Deconvolution algorithms			
		FSD	SBD	BD-ATV	BD-SMR
FWHMR	3-Pentanol	1.65	2.26	2.98	**4.36**
	Butyl Formate	1.46	2.16	2.63	**3.22**
	Cumene	1.39	2.36	2.61	**2.98**
NAR	3-Pentanol	1.69	1.96	2.18	**2.37**
	Butyl Formate	1.44	1.76	1.85	**2.28**
	Cumene	1.37	1.59	1.83	**2.01**

B. Real Experiments

In addition, we test the effectiveness of the proposed algorithm on real spectra. In order to save space, only two of them are illustrated. In Fig. 6, we show the recovered results by different methods on the infrared spectrum of L(+)-Arabinofuranose ($C_5H_{10}O_5$). The random noise and band overlap (marked in red arrows) are existed in the degraded spectrum. The proposed method produces a more visually pleasing result, compared with the results of other methods. As indicated by the mark in Fig. 5(b), the FSD method has not split the overlap band at 860 cm-1. The residual noise is also observed in Fig. 5(c) by BD-ATV method. Indices NAR and FWHMR, as listed in Table III, show that our method has achieved the best performance among the tested methods.

Visual inspection shows that our method outperforms the compared methods with respect to reducing noise and preserving the band information. Table III shows all the NAR and FWHMR values of all the six spectra. It is seen that all the deconvolution methods raise the indexes, but the proposed method obtains the highest values for the six spectra.

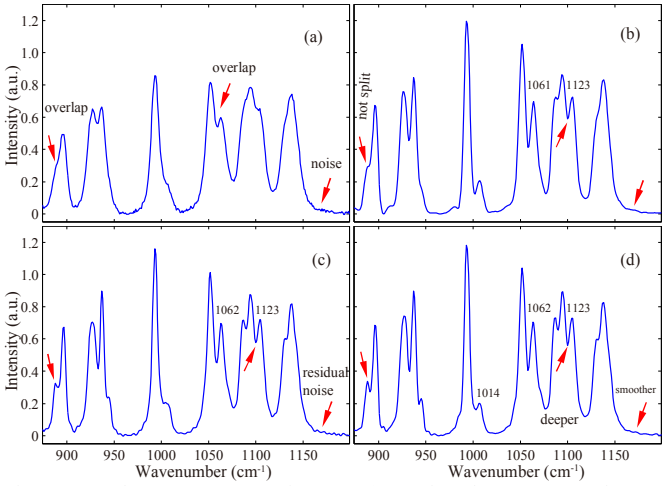

Fig. 6. Real spectrum experiments. (a) Infrared spectrum of L(+)-Arabinofuranose ($C_5H_{10}O_5$). (b) FSD method [11]. (c) BD-ATV method [18]. (d) BD-SWR method.

Table III. FWHMR and NAR (in Bracket) values of different deconvolution methods on the real IR spectra. The larger the value of FWHMR and NAR, the higher the spectral quality.

Spectra	FSD	SBD	BD-ATV	BD-SMR
L(+)-Arabinofuranose	1.85 (1.42)	2.26 (1.78)	2.93 (2.30)	**3.10 (2.42)**
IR 2	1.46 (1.89)	1.68 (2.10)	2.30 (2.41)	**2.51 (2.55)**
IR 3	1.34 (1.21)	2.07 (1.73)	2.12 (1.79)	**2.46 (2.04)**
IR 4	1.84 (1.39)	2.19 (1.77)	2.92 (2.30)	**3.08 (2.46)**
IR 5	1.58 (1.49)	1.72 (1.68)	2.26 (1.96)	**2.66 (2.22)**
IR 6	1.95 (1.69)	2.37 (1.89)	2.84 (2.15)	**3.24 (2.67)**

VI. CONCLUSIONS

In this paper, we propose an effective spectral deconvolution method with similarity of multi-scales regularization. The method first downsamples the degraded spectrum to each scales, and then make use of the similarity of adjacent scales as a constraint to recover the overlap spectrum at each scales. Experimental results show that the proposed method could estimate more accurate instrument function and obtain better performance than the state-of-the-art methods, and the proposed method could get more details with less artifacts. The deconvolution infrared spectra can easily extract the spectral features and interpret the unknown material. Although the application considered here is infrared spectrum, the proposed method is more general applicable to other spectrum lines.

ACKNOWLEDGMENT

The authors thank the editor and anonymous reviewers for their valuable suggestions. This research was partially funded by the National Social Science Fund of China (14BGL131), the Self-determined Research Funds of CCNU from the Colleges' Basic Research and Operation of MOE (CCNU15A05059, CCNU15A05009, CCNU15A05010), the National Natural Science Foundation of China under Grant (No. 61505064), the Project of the Program for National Key Technology Research and Development Program (2013BAH72B01, 2013BAH18F02, 2015BAH33F02), Scientific R&D Project of State Education Ministry and China Mobile (MCM20121061), New PhD Researcher Award from Chinese Ministry of Education, and New Century Excellent Talents in University (NCET-11-0654).

REFERENCES

[1] Q. Gao, D. Zhu, D. Sun, and Y. Lu, "A denoising method based on null space pursuit for infrared spectrum," *Neurocomputing,* vol. 137, no. 0, pp. 180-184, 2014.

[2] N. B. Colthup, L. H. Daly, and S. E. Wiberley, *Introduction to infrared and Raman spectroscopy*, New York: Academic press, 1990.

[3] A. Barth, "Infrared spectroscopy of proteins," *Biochimica et Biophysica Acta (BBA) - Bioenergetics,* vol. 1767, no. 9, pp. 1073-1101, 2007.

[4] A. L. Gallego, A. R. Guesalaga, E. Bordeu, Gonza, x, and A. S. lez, " Rapid Measurement of Phenolics Compounds in Red Wine Using Raman Spectroscopy," *Instrumentation and Measurement, IEEE Transactions on,* vol. 60, no. 2, pp. 507-512, 2011.

[5] H. Liu, L. Yan, Y. Chang, H. Fang, and T. Zhang, "Spectral deconvolution and feature extraction with robust adaptive Tikhonov regularization," *IEEE Transactions on Instrumentation and Measurement,* vol. 62, no. 2, pp. 315-327, 2013.

[6] J. Ma, J. Zhao, J. Tian, Y. A. L., and Z. Tu, "Robust Point Matching via Vector Field Consensus," *Image Processing, IEEE Transactions on,* vol. 23, no. 4, pp. 1706-1721, 2014.

[7] J. R. Riba Ruiz, T. Canals, and R. Cantero Gomez, "Comparative Study of Multivariate Methods to Identify Paper Finishes Using Infrared Spectroscopy," *Instrumentation and Measurement, IEEE Transactions on,* vol. 61, no. 4, pp. 1029-1036, 2012.

[8] J. Ma, W. Qiu, J. Zhao, Y. Ma, Y. A. L., and Z. Tu, "Robust L2E Estimation of Transformation for Non-Rigid Registration," *Signal Processing, IEEE Transactions on,* vol. 63, no. 5, pp. 1115-1129, 2015.

[9] K. Zhang, and L.-W. Chan, "Convolutive blind source separation by efficient blind deconvolution and minimal filter distortion," *Neurocomputing,* vol. 73, no. 13–15, pp. 2580-2588, 2010.

[10] Y. Shen, J. Li, Z. Zhu, W. Cao, and Y. Song, "Image reconstruction algorithm from compressed sensing measurements by dictionary learning," *Neurocomputing,* vol. 151, Part 3, no. 0, pp. 1153-1162, 2015.

[11] V. A. Lórenz-Fonfría, and E. Padrós, "The Role and Selection of the Filter Function in Fourier Self-Deconvolution Revisited," *Appl. Spectrosc.,* vol. 63, no. 7, pp. 791-799, 2009.

[12] J. K. Kauppinen, D. J. Moffatt, H. H. Mantsch, and D. G. Cameron, "Fourier Self-Deconvolution: A Method for Resolving Intrinsically Overlapped Bands," *Appl. Spectrosc.,* vol. 35, no. 3, pp. 271-276, 1981.

[13] L. Yan, H. Liu, S. Zhong, and H. Fang, "Semi-blind spectral deconvolution with adaptive Tikhonov regularization," *Applied Spectroscopy,* vol. 66, no. 11, pp. 1334-1346, 2012.

[14] H. Liu, T. Zhang, L. Yan, H. Fang, and Y. Chang, "A MAP-based algorithm for spectroscopic semi-blind deconvolution," *Analyst,* vol. 137, no. 16, pp. 3862-3873, 2012.

[15] S. Sarkar, P. K. Dutta, and N. C. Roy, "A blind-deconvolution approach for chromatographic and spectroscopic peak restoration," *Instrumentation and Measurement, IEEE Transactions on,* vol. 47, no. 4, pp. 941-947, 1998.

[16] J. Yuan, and Z. Hu, "High-Order Statistical Blind Deconvolution of Spectroscopic Data with a Gauss-Newton Algorithm," *Appl. Spectrosc.,* vol. 60, no. 6, pp. 692-697, 2006.

[17] H. Liu, M. Zhou, Z. Zhang, J. Shu, T. Liu, and T. Zhang, "Multi-order blind deconvolution algorithm with adaptive Tikhonov regularization for infrared spectroscopic data," *Infrared Physics & Technology,* vol. 71, pp. 63-69, 2015.

[18] H. Liu, S. Liu, Z. Zhang, J. Sun, and J. Shu, "Adaptive total variation-based spectral deconvolution with the split Bregman method," *Applied Optics,* vol. 53, no. 35, pp. 8240-8248, 2014.

[19] V. A. Lórenz-Fonfría, and E. Padrós, "Maximum Entropy Deconvolution of Infrared Spectra: Use of a Novel Entropy Expression Without Sign Restriction," *Appl. Spectrosc.,* vol. 59, no. 4, pp. 474-486, 2005.

[20] H. Liu, Z. Zhang, J. Sun, and S. Liu, "Blind spectral deconvolution algorithm for Raman spectrum with Poisson noise," *Photonics Research,* vol. 2, no. 6, pp. 168-171, 2014.

[21] H. Liu, Z. Zhang, S. Liu, T. Liu, L. Yan, and T. Zhang, "Richardson-Lucy blind deconvolution of spectroscopic data with wavelet regularization," *Applied Optics,* vol. 54, no. 7, pp. 1770-1775, 2015.

[22] H. Liu, Z. Zhang, S. Liu, Z. Yan, and T. Liu, "Band Narrowing with Sparsity Regularization for Spectroscopic Data," in 2015 5th IEEE International Conference on Information Science and Technology (ICIST 2015), Changsha, China, April 24-26, 2015, pp. 165-172.

[23] P. R. Griffiths, and L. Shao, "Self-Weighted Correlation Coefficients and Their Application to Measure Spectral Similarity," *Appl. Spectrosc.,* vol. 63, no. 8, pp. 916-919, 2009.

[24] J. KatraSnik, F. Pernu, and B. t. Likar, "Deconvolution in Acousto-Optical Tunable Filter Spectrometry," *Applied Spectroscopy,* vol. 64, no. 11, pp. 1265-1273, 2010.

[25] H. Liu, Z. Zhang, S. Liu, J. Shu, T. Liu, and T. Zhang, "Blind spectrum reconstruction algorithm with L0-sparse representation," *Measurement Science and Technology,* vol. 26, no. 8, pp. 085502, 2015.